Air-ground Trajectory Tracking for Discrete-Time Autonomous Mobile Robot Based on Model Predictive Hybrid Tracking Control and Multiple Harmonics Time-varying Disturbance Observer

Shixun Xiong (xgybq321@njupt.edu.cn)
Nanjing University of Posts and Telecommunications https://orcid.org/0000-0002-8683-9362
Mengting Chen
Nanjing University of Posts and Telecommunications
Ziqiang Wei
Nanjing University of Posts and Telecommunications

Research Article

Keywords: Autonomous mobile robot, air-ground tracking, discrete-time system, model predictive control, nonholonomic constraints

Posted Date: April 11th, 2022

DOI: https://doi.org/10.21203/rs.3.rs-1480180/v1

Noname manuscript No.
(will be inserted by the editor)

Air-ground Trajectory Tracking for Discrete-Time Autonomous Mobile Robot Based on Model Predictive Hybrid Tracking Control and Multiple Harmonics Time-varying Disturbance Observer

Shixun Xiong · Mengting Chen · Ziqiang Wei

Received: date / Accepted: date

Abstract This paper studies a model predictive hybrid tracking control scheme under a multiple harmonics time-varying disturbance observer for a discrete-time dynamics nonholonomic autonomous mobile robot (AMR) with external disturbance. To solve the robust tracking control problem of the AMR and unmanned aerial vehicle (UAV) air-ground cooperative, a hybrid tracking control strategy combined with improved model predictive control (MPC) method and multiple harmonics time-varying disturbance observer is presented. Firstly, a time-varying air-ground cooperative tracking control model based on the nonholonomic constraints AMR and quadrotor is established by polar coordinate transformation. Secondly, for external disturbances estimating and solving in practical engineering, a discrete-time multiple harmonics time-varying disturbance observer is designed. A hybrid tracking control scheme of the AMR based on the estimated states and MPC method with kinematics constraints is proposed, and a relaxing factor is designed to restrain the jump phenomenon of the MPC increment. Finally, experimental results are shown the effectiveness of the proposed control strategy.

Shixun Xiong
Jiangsu Key Laboratory of Broadband Wireless Communication and Internet of Things, School of Internet of Things, Nanjing University of Posts and Telecommunications, Nanjing 210003, China
E-mail: xgybq321@njupt.edu.cn

Mengting Chen
Jiangsu Key Laboratory of Broadband Wireless Communication and Internet of Things, School of Internet of Things, Nanjing University of Posts and Telecommunications, Nanjing 210003, China
E-mail: 403998958@qq.com

Ziqiang Wei
Jiangsu Key Laboratory of Broadband Wireless Communication and Internet of Things, School of Internet of Things, Nanjing University of Posts and Telecommunications, Nanjing 210003, China
E-mail: leonlew@139.com

Keywords Autonomous mobile robot · air-ground tracking · discrete-time system · model predictive control · nonholonomic constraints

1 Introduction

Autonomous mobile robots (AMRs) and unmanned aerial vehicles (UAVs) can implement many complex air-ground cooperation tasks, such as surveillance, rescue, and transportation. With the development of electronic technology, the movement speed and real-time control performance of AMRs cooperation motion have higher requirements [1]. However, since the nonlinear characteristic of the AMR system with nonholonomic constraints, it is difficult to establish an effective cooperative tracking control model for the AMR and UAV, which increases the complexity of the real-time control strategy designing [2]. Besides, for the AMR and UAV cooperative tracking, the external disturbance often exists in AMR and UAV simultaneously in the form of multiple harmonics, which affects the maneuverability of cooperative tracking control performance. Therefore, based on the nonlinear AMR and UAV system, a new air-ground tracking frame and effective robust tracking control scheme is necessary to complement the cooperation tasks with external disturbance.

The air-ground tracking control problem has received considerable interest for many applications, such as collaborative path planning and trajectory tracking [3]- [6]. In the air-ground trajectory tracking process, the establishment of cooperative control model will affect the controller designing. Combined with the data fusion technology, an air-ground cooperation frame through the environment awareness was proposed for AMRs tracking [7]. To enhance control performance can cope with more complex practical cooperative tracking tasks [8]. Under the uncertainties parameters and actuator faults, a UAV-UGV cooperative control scheme was presented for the formation cooperative finite-time trajectory tracking control [9]. In [10], combined with continuous-time dynamics of a wheeled mobile robot (WMR), a cooperative control scheme was designed based on the information sharing and data fusion technology for the air-ground tracking. With the development of industrial control technology, the discrete-time dynamics AMR system in practical engineering increased the complexity of the controller designing by comparing with the continuous-time system. Therefore, to overcome these issues of the AMR and obtain an effective tracking control scheme, the problems of the discrete-time dynamics AMR tracking control analysis should be considered.

It should be noted that the tracking control of AMRs is a complex problem with internal constraints, such as nonholonomic constraints and actuator saturation [11]. The tracking control scheme under these constraints can be designed based on a model predictive control (MPC) method, which is a receding horizon control method to handle constraints through optimization procedures [12]-[14]. In [15], a trajectory tracking control strategy under the MPC method applied to an omni-directional AMR was investigated. Based on the multiple nonholonomic AMRs, a nonlinear MPC scheme for the collision-free and deadlock-free navigation tracking was presented with a desired target [16]. In [17], a vision-based MPC scheme for a nonholonomic mobile robot was proposed to reduce the algorithm complexity. To improve the system tracking accuracy, an MPC method with quadratic robustness constraints of the WMR with incremental input constraints was designed to obtain the optimal tracking control scheme [18]. However, based on the MPC method, the tracking control problem of the AMR with the constraint conditions is transferred into a linear quadratic programming problem, which is difficult to handle for the discrete-time nonlinear dynamics AMR system. Besides, although the control scheme can be generally solved by an MPC optimization algorithm, the external disturbance will decrease the tracking performance of AMRs in practical engineering. Therefore, a disturbance attenuation method should be considered to achieve the optimal solution of the control input for AMRs trajectory tracking.

The disturbance observer was widely used as a feedforward compensation method to handle the external disturbance of systems in recent years [19]-[21]. In [22], combined with compound disturbance, a nonlinear-disturbance-observer-enhanced control scheme based on a nonlinear disturbance observer was studied for the motion control system. However, Under the nonholonomic constraints characteristics of the AMR, the system dynamics of the AMR are nonlinear, and the system parameters are time-varying, which increases the design difficulty of the disturbance observer. Considering the input disturbance, a robust control strategy was presented for the WMR with nonlinear disturbance observer [11]. Nevertheless, the stability analysis of the MPC method is different from the general method under the disturbance observer [23]. A disturbance rejection MPC scheme under the nonlinear disturbance observer was investigated for the tracking control of the continuous-time dynamics WMR [24]. In practical situation, most disturbances are composed of different frequency harmonics, which can be estimated separately for state compensation of systems, hence the multiple harmonics disturbance observer has been studied [25]. However, considering the nonlinear time-varying dynamics of the discrete-time dynamics AMR, the gain parameters of the disturbance observer may be time-varying simultaneously. Therefore, to design a discrete-time time-varying disturbance observer for the multiple harmonics disturbance attenuation and rejection of the AMR tracking is worth to be considered.

A hybrid tracking control strategy under an improved MPC method and a time-varying multiple harmonics disturbance observer is proposed for a discrete-time AMR in this paper. The main contributions lie in:

1) To perform the cooperative tracking control of the AMR and UAV, a discrete-time dynamics nonlinear time-varying tracking model is established under the nonholonomic AMR and quadrotor by horizontal projection and polar coordinate transformation method. Besides, considering the external disturbance composed of different frequency harmonics, a multiple harmonics time-varying disturbance observer is presented for the nonlinear tracking model for disturbance estimation, and the time-varying gains of the distur-

bance observer are solved by the proposed MPC method in this paper, which conforms to practical applications.

2) The difference between the traditional model predictive tracking control strategy and the designed one of this paper is that the tracking control scheme consists of feedforward compensation items generated by the multiple harmonics time-varying disturbance observer and feedback control inputs generated by the MPC method, and the relax factor is introduced for MPC method improving to restrain the jump phenomenon of the MPC increment and ensure the stability of the MPC feasible solutions. Furthermore, using the improved MPC method to solve the time-varying gains of the disturbance observer, an experiment is carried out for the AMR to verify the effectiveness of the proposed control strategy.

This paper is organized as follows: Section II presents the establishment of the nonlinear discrete-time cooperative tracking model of the AMR and UAV, and the multiple harmonics disturbance observer is designed. In Section III, the hybrid tracking control scheme based on the disturbance observer and MPC method with relaxing factor is designed, and the stability analysis is given. The experimental results with the AMR are shown in Section IV. Section V summarizes the conclusion.

2 Problem Formulation

2.1 The establishment of tracking control model

In the partial air-ground cooperative tracking tasks, the trajectory motion of the AMR is usually guided by the UAV, especially quadrotor. With the characteristics of flexibility and light, quadrotor is convenient to perform cooperative tasks with the AMR, and its height can be independently controlled so that the quadrotor can fly to a specified altitude [25]. Besides, the research of the cooperation of the AMR and UAV mainly focuses on trajectory tracking, and there is no control over the pitch and roll angle of the AMR when tracking the UAV. Therefore, this work focuses on the controller design and stability analysis of the AMR trajectory tracking control in the horizontal plane. Inspired by Ref. [26], the AMR can track the UAV trajectory projection on the ground. Then considering the nonholonomic constraints and UAV trajectory projection tracking of the AMR, the trajectory of the UAV can be converted into the trajectory satisfying the motion constraints of the AMR when the AMR tracks the UAV. The air-ground tracking process is depicted in Fig. 1.

The projection of the air-ground tracking of the AMR and UAV is depicted in Fig. 2. From Fig. 2, the AMR is driven by two wheels at the bottom, and the ground coordinate is denoted as XOY. Choosing O as the reference point, the controlled AMR position P and the UAV position P_r in the ground coordinate XOY are defined as $o(x, y)$ and $o_r(x_r, y_r)$, respectively, where x, x_r and y, y_r are the transverse and vertical coordinates of P and P_r. θ and θ_r are the angles between OX axis and symmetry axis. The linear velocity of the AMR in point

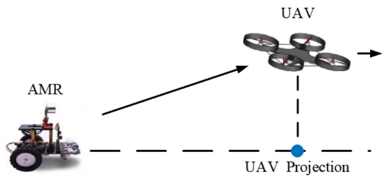

Fig. 1: The air-ground tracking with AMR and UAV

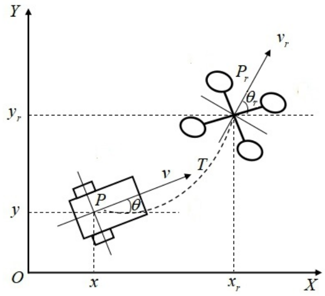

Fig. 2: The projection of the air-ground tracking

(x, y) is v, and w is the angular rate. v_r and w_r are the linear velocity and angular rate of the UAV.

Define the position of the AMR as $\eta(k) = [x(k), y(k), \theta(k)]^T$. Then, the nonlinear discrete-time dynamics of a nonholonomic AMR with two actuated wheels can be described as follows [27]:

$$\begin{aligned} x(k+1) &= x(k) + v(k) \cdot \cos\theta(k) \cdot T \\ y(k+1) &= y(k) + v(k) \cdot \sin\theta(k) \cdot T \\ \theta(k+1) &= \theta(k) + w(k) \cdot T \end{aligned} \tag{1}$$

where the linear velocity is $v(k)$ and angular rate is $w(k)$. $T(0 < T < 1)$ is the sample interval.

For practical tasks, to complement AMR real-time tracking, the UAV will transfer the dynamic trajectory of itself into the AMR, which guarantees the trajectory tracking real-time of the AMR. Besides, combined with Ref. [26], to complement the AMR trajectory tracking, the dynamic trajectory of the UAV can be projected on the ground and converted into the trajectory satisfying the motion constraints of the AMR. Therefore, a projected trajectory dynamic of the discrete-time UAV system on the ground is described as follows [28]:

$$\begin{aligned} x_r(k+1) &= x_r(k) + v_r(k)\cos\theta_r(k)T \\ y_r(k+1) &= y_r(k) + v_r(k)\sin\theta_r(k)T \\ \theta_r(k+1) &= \theta_r(k) + w_r(k)T \end{aligned} \tag{2}$$

where x_r, y_r and θ_r are position and heading angle of the UAV projection, respectively, which is shown in Fig. 2. v_r and w_r are the corresponding linear velocity and angular rate.

To complete the trajectory tracking in the projected horizontal plane, the tracking error of the AMR is defined that

$$\begin{array}{l} x_e(k) = x(k) - x_r(k) \\ y_e(k) = y(k) - y_r(k) \\ \theta_e(k) = \theta(k) - \theta_r(k) \end{array} \tag{3}$$

For the AMR tracking error model, most previous works were localized with a Cartesian set of variables. However, different from the continuous-time AMR model, the analysis and the controller design for discrete-time AMR tracking error model is more complex and challenging. Therefore, inspired by Ref. [17], the tracking error (3) can be transformed from Cartesian coordinates into polar coordinates, which is helpful for designing the tracking control scheme of the discrete-time AMR. The tracking error variables with the polar coordinate system are shown in Fig. 3. Under the UAV projected states x_r, y_r and θ_r, the tracking error based on the polar coordinate system is defined as

$$\begin{array}{l} e(k) = \sqrt{(x_r - x)^2 + (y_r - y)^2} \\ \phi(k) = \arctan\left(-(x_r - x), -(y_r - y)\right) \end{array} \tag{4}$$

where $e(k)$ is the distance between the AMR and UAV projection in the polar coordinates, $\phi(k)$ is the angle between the desired direction and OX axis. Let $\alpha(k)$ as the angle between the current motion direction and the desired position, the tracking error system under the polar coordinates of the AMR is depicted as

$$\begin{array}{l} e(k) = \sqrt{x_e^2(k) + y_e^2(k)} \\ \phi(k) = \arctan(-y_e(k), -x_e(k)) \\ \alpha(k) = \phi(k) - \theta(k) \end{array} \tag{5}$$

where $x_e(k) = e(k)\cos\phi(k)$ and $y_e(k) = e(k)\sin\phi(k)$, α and ϕ are shown in Fig. 3.

Invoking (1), (4), (5) and Fig. 3, the tracking errors $e(k)$ and $\theta_e(k)$ can be transformed as follows [17]:

$$\begin{aligned} e(k+1) &= e(k) - v(k)\cos\alpha(k)T \\ \theta_e(k+1) &= \theta(k) + w(k)T - \theta_r(k) - w_r(k)T \\ &= \theta_e(k) - w_r(k)T + w(k)T \end{aligned} \tag{6}$$

Considering that during the movement, the position of the AMR will be affected under external disturbance. Therefore, invoking with (6), a polar coordinate tracking error model of the AMR with external disturbance is described as follows:

$$\begin{array}{l} e(k+1) = e(k) - v(k)\cos\alpha(k)T + d(k) \\ \theta_e(k+1) = \theta_e(k) - w_r(k)T + w(k)T + d(k) \end{array} \tag{7}$$

where $d(k)$ is the external disturbance.

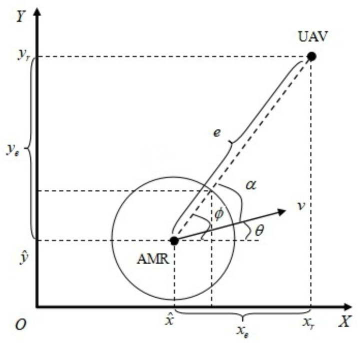

Fig. 3: AMR tracking under polar coordinate system

The control objective is to design a tracking control scheme for the AMR such that the AMR (1) can track the UAV projection trajectory (2) under the external disturbance. To design the AMR tracking control scheme, the following assumptions are considered.

Assumption 1 [29]: The system state of the AMR is measurable, and there is no slipping and skidding in the AMR.

Assumption 2 [30]: The angle between the desired direction direction and the current motion is bounded, such that $-\frac{\pi}{2} < \phi - \theta < \frac{\pi}{2}$.

Remark 1 In Assumption 2, the AMR can adjust its motion direction preferentially in the practical tracking process. If the angle between the desired position and the current motion direction is too large, the AMR can firstly adjust its motion direction to make it forward direction close to the desired position, which reduces the angle difference between the motion direction and the desired position, and then continues to track.

Invoking (3) and (5), we have

$$\begin{aligned}\alpha(k) &= \phi(k) - \theta(k)\\ \theta(k) &= \theta_r(k) - \theta_e(k)\end{aligned} \tag{8}$$

According to (7) and (8), the tracking error $e(k)$ can be written as follows:

$$\begin{aligned}e(k+1) &= e(k) - v(k)\cos\left(\phi(k) - \theta(k)\right)T + d(k)\\ &= e(k) - v(k)\left(\cos\phi(k)\cos\theta(k)\right.\\ &\quad\left. + \sin\phi(k)\sin\theta(k)\right)T + d(k)\\ &= e(k) - v(k)\left[\cos\phi(k)\cos\left(\theta_r(k) - \theta_e(k)\right)\right.\\ &\quad\left. + \sin\phi(k)\sin\left(\theta_r(k) - \theta_e(k)\right)\right]T + d(k)\\ &= e(k) - v(k)\cos\phi(k)\cos\theta_r(k)\cos\theta_e(k)T\\ &\quad - v(k)\cos\phi(k)\sin\theta_r(k)\sin\theta_e(k)T\\ &\quad - v(k)\sin\phi(k)\sin\theta_r(k)\cos\theta_e(k)T\\ &\quad + v(k)\sin\phi(k)\cos\theta_r(k)\sin\theta_e(k)T + d(k)\end{aligned} \tag{9}$$

Invoking (7) and (9), we have

$$\begin{bmatrix} e(k+1) \\ \theta_e(k+1) \end{bmatrix} = \begin{bmatrix} e(k)+p_1(k)+d(k) \\ \theta_e(k)-w_r(k)T+w(k)T+d(k) \end{bmatrix} \tag{10}$$

where

$$\begin{aligned} p_1(k) = {} & v(k)\sin\phi(k)\cos\theta_r(k)\sin\theta_e(k)T \\ & -v(k)\cos\phi(k)\sin\theta_r(k)\sin\theta_e(k)T \\ & -v(k)\sin\phi(k)\sin\theta_r(k)\cos\theta_e(k)T \\ & -v(k)\cos\phi(k)\cos\theta_r(k)\cos\theta_e(k)T \end{aligned} \tag{11}$$

Letting $p(k) = [e(k), \theta_e(k)]^T$ and $u(k) = \left[v^T(k), w^T(k) \right]^T$, a discrete-time time-varying error system under equation (10) is given in the following form

$$p(k+1) = F(p(k)) + G(p(k))u(k) + Dd(k) \tag{12}$$

where

$$\begin{aligned} & F(p(k)) = \begin{bmatrix} e(k) \\ \theta_e(k)-w_r(k)T \end{bmatrix} \\ & G(p(k)) = \begin{bmatrix} TG_1(p(k)) & 0 \\ 0 & T \end{bmatrix} \\ & D = \begin{bmatrix} 1 \; 1 \end{bmatrix}^T \\ & G_1(p(k)) = \sin\phi(k)\cos\theta_r(k)\sin\theta_e(k) \\ & \qquad -\cos\phi(k)\sin\theta_r(k)\sin\theta_e(k) \\ & \qquad -\sin\phi(k)\sin\theta_r(k)\cos\theta_e(k) \\ & \qquad -\cos\phi(k)\cos\theta_r(k)\cos\theta_e(k) \end{aligned} \tag{13}$$

Then, to design the multiple harmonics disturbance observer of the AMR, the following assumption is considered.

Assumption 3 [31]: For system (12), the time-varying disturbance can be formed by the following linear exogenous system:

$$\begin{aligned} & \varsigma_i(k+1) = Z_i\varsigma_i(k) \\ & d(k) = \sum_{i=1}^{n} M_i\varsigma_i(k) \end{aligned} \tag{14}$$

where $\varsigma_i(k)$ are the auxiliary variables of disturbances, Z_i and M_i are the known matrices.

2.2 Multiple harmonics time-varying disturbance observer

For the continuous-time dynamics AMR, the disturbance observer technique has been widely studied by researchers. However, the tracking error model (12) of the AMR is discrete-time dynamics and time-varying, and the disturbance $d(k)$ is composed of multiple harmonics, which increases the difficulty in the design of the disturbance observer. Therefore, a discrete-time linear time-varying multiple harmonics disturbance observer is designed to estimate each harmonic disturbance respectively. Here we define

$$\begin{aligned}
&\hat{d}(k) = \sum_{i=1}^{N} M_i \varsigma_i(k) \\
&\hat{\varsigma}_1(k) = \eta_1(k) - L_1(k)p(k) \\
&\hat{\varsigma}_2(k) = \eta_2(k) - L_2(k)p(k) \\
&\vdots \\
&\hat{\varsigma}_N(k) = \eta_N(k) - L_N(k)p(k)
\end{aligned} \tag{15}$$

where $\eta_i(k)$ are the auxiliary variables, $\hat{\varsigma}_i(k)$ and $\hat{d}(k)$ are the estimated values of $\varsigma_i(k)$ and $d(k)$, respectively. $L_i(k)$ are the designed time-varying gains of the disturbance observer.

Then, to estimate $d(k)$, a multiple harmonics time-varying disturbance observer is developed as follows:

$$\begin{aligned}
\eta_i(k+1) = &(Z_i + L_i(k)DM_i)\hat{\varsigma}_i(k) \\
&+L_i(k)[F(p(k)) + G(p(k))u(k) \\
&+D\sum_{j=1}^{i-1} M_j\hat{\varsigma}_j(k) + D\sum_{j=i+1}^{N} M_j\hat{\varsigma}_j(k)] \\
\hat{\varsigma}_i(k) = &\eta_i(k) - L_i(k)p(k) \\
\hat{d}_i(k) = &\sum_{i=1}^{N} M_i\hat{\varsigma}_i(k)
\end{aligned} \tag{16}$$

Define the estimated errors as

$$e_{\varsigma_i}(k) = \varsigma_i(k) - \hat{\varsigma}_i(k) \tag{17}$$

Invoking (14), (15), (16) and (17), it yields

$$\begin{aligned}
e_{\varsigma_i}(k+1) &= \varsigma_i(k+1) - \hat{\varsigma}_i(k+1) \\
&= Z_i\varsigma_i(k) - \eta_i(k+1) + L_i(k+1)p(k+1) \\
&= Z_i\varsigma_i(k) - (Z_i + L_i(k)DM_i)\hat{\varsigma}_i(k) \\
&\quad -L_i(k)[F(p(k)) + G(p(k))u(k) \\
&\quad +D\sum_{j=1}^{i-1} M_j\hat{\varsigma}_j(k) + D\sum_{j=i+1}^{N} M_j\hat{\varsigma}_j(k)] \\
&\quad +L_i(k)[F(p(k)) + G(p(k))u(k) + Dd(k)] \\
&= Z_i(\varsigma_i(k) - \hat{\varsigma}_i(k)) - L_i(k)DM_i\hat{\varsigma}_i(k) \\
&\quad -D\sum_{j=1}^{i-1} M_j\hat{\varsigma}_j(k) - D\sum_{j=i+1}^{N} M_j\hat{\varsigma}_j(k) \\
&\quad +L_i(k)Dd(k) \\
&= Z_i e_{\varsigma_i}(k) + L_i(k)D\sum_{j=1}^{N} M_j e_{\varsigma_j}(k)
\end{aligned} \tag{18}$$

Defining the augment vectors as $e_\varsigma^T = \left[e_{\varsigma_1}^T, e_{\varsigma_2}^T, ..., e_{\varsigma_N}^T\right]$, $L^T = \left[L_1^T, L_2^T, ..., L_N^T\right]$, $M = [M_1, M_2, ..., M_N]$ and $Z = [Z_1, Z_2, ..., Z_N]$, equation (18) can be rewritten as

$$\begin{aligned}
e_\varsigma(k+1) &= Ze_\varsigma(k) + L(k)DMe_\varsigma(k) \\
&= (Z + L(k)DM)e_\varsigma(k)
\end{aligned} \tag{19}$$

Based on the multiple harmonics time-varying disturbance observer, a hybrid tracking control scheme under the MPC method is designed for trajectory tracking accurately in the next section.

3 Design of The Tracking Control Scheme

In this section, to obtain the time-varying gains of disturbance observer and guarantee cooperative tracking performance of the AMR, a hybrid tracking control scheme based on the MPC method with relaxing factor and the disturbance estimated values is proposed.

3.1 The hybrid control scheme

Based on (8), (9), (12) and (13), the term $G\left(p(k)\right)$ is related to α and $\alpha = \phi - \theta$. According to Assumption 2, it has $-\frac{\pi}{2} < \phi - \theta < \frac{\pi}{2}$, which yields that $0 < \cos\alpha < 1$. Then it induces that $G_1(p(k)) \neq 0$ and $G(p(k))$ is an nonsingular matrix. Hence, it can obtain a time-varying matrix $\tilde{G}(p(k))$ which satisfy $G(p(k))\tilde{G}(p(k)) = D$. Then, for error system (12), the control scheme $u(k)$ can be designed as $u(k) = u_m(k) - u_d(k)$, where $u_d(k)$ is the feedforward compensation term of the control input after obtaining the estimated values of the disturbance observer and $u_d(k) = \tilde{G}(p(k))\hat{d}(k)$, $u_m(k)$ is the feedback control input, and $u_m(k)$ and $L_i(k)$ will be calculated by MPC method, which constitute the hybrid control input. Therefore, system (12) can be rewritten as

$$\begin{aligned} p(k+1) &= F(p(k)) + G(p(k))(u_m(k) - u_d(k)) + Dd(k) \\ &= G(p(k))(u_m(k) - \tilde{G}(p(k))\hat{d}(k)) \\ &\quad + F(p(k)) + Dd(k) \\ &= F(p(k)) + G(p(k))u_m(k) - D\hat{d}(k) + Dd(k) \\ &= F(p(k)) + G(p(k))u_m(k) - DMe_\varsigma(k) \end{aligned} \tag{20}$$

Combined with $p(k)$ and $e_\varsigma(k)$, letting $\bar{p}(k) = \left[e^T(k), \theta_e^T(k), e_\varsigma^T(k)\right]^T$, equation (20) can be given by

$$\bar{p}(k+1) = \bar{F}(\bar{p}(k)) + \bar{G}(\bar{p}(k))u_m(k) + \bar{L}(k)e_\varsigma(k) \tag{21}$$

where

$$\bar{F}(\bar{p}(k)) = \begin{bmatrix} e(k) \\ \theta_e(k) - w_r(k)T \\ Ze_\varsigma(k) \end{bmatrix}, \bar{L}(k) = \begin{bmatrix} -M \\ -M \\ L(k)DM \end{bmatrix}$$
$$\bar{G}(\bar{p}(k)) = \begin{bmatrix} TG_1(p(k)) & 0 \\ 0 & T \\ 0 & 0 \end{bmatrix}$$

Remark 2 For (21), if the state of the system (21) is convergent, then the disturbance estimation errors and the trajectory errors are convergent. In addition, the closed-loop system constructed in the form of equation (21) is convenient to use the MPC method to obtain the feedback control input u_m, and also to get the time-varying gain matrix $L(k)$ of the disturbance observer by the MPC method.

3.2 The design of MPC method with relaxing factor

The MPC method is an iterated solution online of an optimization problem, which can be introduced to obtain the tracking control scheme with constraints. It means that the feedback control input $u_m(k)$ and time-varying disturbance observer gain matrix $L(k)$ is obtained through the MPC method. The control input increment solved by traditional MPC method exists jump phenomenon, hence in this paper the relax factor is introduced for MPC method to restrain the jump phenomenon of the increment and ensure the stability of the MPC feasible solutions. From (21), with soft constraints, a cost function is given as follows [29]:

$$
\begin{aligned}
J(k) = &\sum_{\vartheta=1}^{n} \bar{p}^T(k+\vartheta|k)V\bar{p}(k+\vartheta|k) \\
&+\sum_{\vartheta=0}^{n-1} \Delta u_m^T(k+\vartheta|k)Y\Delta u_m(k+\vartheta|k) \\
&+\sum_{\vartheta=0}^{n-1} \gamma^T(k+\vartheta|k)W\gamma(k+\vartheta|k)
\end{aligned} \tag{22}
$$

where $\bar{p}(k+\vartheta|k)$ and $\Delta u_m(k+\vartheta|k)$ denotes the predicted state and control input increment in the future horizon, n is the predicted horizon, $\gamma(k+\vartheta|k)$ is the relaxing factor, which ensures to obtain the MPC infeasible solutions and restrains the jump phenomenon, the predictive control input increment $\Delta u_m(k+\vartheta|k) = u_m(k+\vartheta|k) - u_m(k+\vartheta-1|k)$. In cost function (22), V, Y and W are the appropriate positive definite matrices. Besides, to avoid the jump phenomenon, the constraints of the state vector $\bar{p}$, the control input u_m and control increment Δu_m are shown as

$$
\begin{aligned}
&\bar{p}_{\min} \leq \bar{p} \leq \bar{p}_{\max} \\
&u_{m_{\min}} \leq u_m \leq u_{m_{\max}} \\
&\Delta u_{m_{\min}} + \gamma c_{\min} \leq \Delta u_m \leq \Delta u_{m_{\max}} + \gamma c_{\max}
\end{aligned} \tag{23}
$$

where $\bar{p}_{\min}$, $\bar{p}_{\max}$, $\Delta u_{m_{\min}}$ and $\Delta u_{m_{\max}}$ are the lower and upper bounds of $\bar{p}$ and Δu_m, respectively. $c_{\min}$ and $c_{\max}$ are the lower and upper bounds of the relaxing factor gain coefficient. The control increment scheme Δu_m is solved through minimizing the cost function (22) with constraints (23). Then the control input scheme u_m is obtained by $u_m(k) = \Delta u_m(k) + u_m(k-1)$. The specific algorithm is described in the following.

According to equations (21) and (22), the predictive vectors are defined as follows:

$$
\begin{aligned}
&\hat{p}(k) = \left[\bar{p}^T(k+1|k), ..., \bar{p}^T(k+n|k)\right]^T \\
&\hat{u}_m(k) = \left[u_m^T(k|k), ..., u_m^T(k+n-1|k)\right]^T \\
&\Delta\hat{u}_m(k) = \left[\Delta u_m^T(k|k), ..., \Delta u_m^T(k+n-1|k)\right]^T \\
&\hat{\gamma}(k) = \left[\gamma^T(k|k), ..., \gamma^T(k+n-1|k)\right]
\end{aligned} \tag{24}
$$

Invoking equations (21) and (24), the predictive vectors can be transformed to state-space equations as

$$
\hat{p}(k) = q(k)\Delta\hat{u}_m(k) + \hat{F}(k) + \hat{G}(k) + \hat{L}(k) \tag{25}
$$

where

$$
\begin{aligned}
&q(k) = \begin{bmatrix} G_1 & 0 & \cdots\cdots & 0 \\ G_2 & G_2 & 0 \ \cdots & 0 \\ G_3 & G_3 & G_3 \ \ddots & 0 \\ \vdots & \vdots & \ddots \ \ddots & \vdots \\ G_{n-1} & G_{n-1} & \cdots\cdots & G_{n-1} \end{bmatrix} \\
&\hat{F}(k) = \begin{bmatrix} \bar{F}(\bar{p}(k|k)) \\ \bar{F}(\bar{p}(k+1|k)) \\ \vdots \\ \bar{F}(\bar{p}(k+n-1|k)) \end{bmatrix} \\
&\hat{L}(k) = \begin{bmatrix} \bar{L}(k|k)e_\varsigma(k|k) \\ \bar{L}(k|k)(Z + L(k|k)DM)e_\varsigma(k|k) \\ \vdots \\ \bar{L}(k|k)(Z + L(k|k)DM)^{n-1}e_\varsigma(k|k) \end{bmatrix} \\
&\hat{G}(k) = \begin{bmatrix} G_1 u_m(k-1) \\ G_2 u_m(k-1) \\ \vdots \\ G_n u_m(k-1) \end{bmatrix} \\
&G_1 = \bar{G}(\bar{p}(k|k)) \\
&G_2 = \bar{G}(\bar{p}(k+1|k)) \\
&\vdots \\
&G_n = \bar{G}(\bar{p}(k+n-1|k))
\end{aligned} \tag{26}
$$

Combined with equations (24), (25) and (26), the cost function (22) subject to constraints (23) becomes

$$
\begin{aligned}
J(k) = &\sum_{\vartheta=1}^{n} \bar{p}^T(k+\vartheta|k)V\bar{p}(k+\vartheta|k) \\
&+ \sum_{\vartheta=0}^{n-1} \Delta u_m^T(k+\vartheta|k)Y\Delta u_m(k+\vartheta|k) \\
&+ \sum_{\vartheta=0}^{n-1} \gamma^T(k+\vartheta|k)W\gamma(k+\vartheta|k) \\
= &\|\hat{p}(k)\|_V^2 + \|\Delta\hat{u}_m(k)\|_Y^2 + \|\hat{\gamma}(k)\|_W^2
\end{aligned} \tag{27}
$$

subject to

$$
\begin{array}{l}
\hat{u}_{\mathrm{m_{min}}} \leq \hat{u}_m(k-1) + I\Delta\hat{u}_m \leq \hat{u}_{\mathrm{m_{max}}} \\
\hat{p}_{\min} \leq \hat{L} + \hat{F} + \hat{G} + q\Delta\hat{u}_m \leq \hat{p}_{\max} \\
\Delta\hat{u}_{m_{\min}} + \hat{\gamma}c_{\min} \leq \Delta\hat{u}_m \leq \Delta\hat{u}_{m_{\max}} + \hat{\gamma}c_{\max}
\end{array}
\tag{28}
$$

where $\bar{V} = diag\{\overbrace{V, ..., V}^{n}\}$, $\bar{Y} = diag\{\overbrace{Y, ..., Y}^{n}\}$ and $\bar{W} = diag\{\overbrace{W, ..., W}^{n}\}$.

Let $\Delta U = \begin{bmatrix} \Delta\hat{u}_m^T & \hat{\gamma}^T \end{bmatrix}^T$ and $\bar{I} = diag\overbrace{\{I, ..., I\}}^{2n}$, the cost function (27) with constraints (28) can be rewritten as a Quadratic Programming (QP) problem

$$
\min \frac{1}{2}\Delta U^T \Xi \Delta U + \Omega^T \Delta U \tag{29}
$$

subject to

$$
E\Delta U \leq \Pi \tag{30}
$$

where the coefficient matrices are

$$
\begin{array}{l}
\Xi = \begin{bmatrix} 2q^T\bar{V}q + 2\bar{Y} & 0 \\ 0 & 2\bar{W} \end{bmatrix}, \Omega = \begin{bmatrix} 2q^T\bar{V}(\hat{G}+\hat{F}) & 0 \\ 0 & 0 \end{bmatrix} \\
E = \begin{bmatrix} \bar{I} & 0 \\ -\bar{I} & 0 \\ q & 0 \\ -q & 0 \\ \bar{I} & c_{\max} \\ -\bar{I} & c_{\min} \end{bmatrix}, \Pi = \begin{bmatrix} \hat{u}_{m_{\max}} - \hat{u}_m(k-1) \\ -\hat{u}_{m_{\min}} + \hat{u}_m(k-1) \\ \hat{p}_{\max} - \hat{F} - \hat{G} - \hat{L} \\ -\hat{p}_{\min} + \hat{F} + \hat{G} + \hat{L} \\ \Delta\hat{u}_{m_{\max}} \\ \Delta\hat{u}_{m_{\min}} \end{bmatrix}
\end{array}
\tag{31}
$$

Remark 3 Combined with equations (27), (29) and (30), to solve the QP problem with constraint conditions, the control schemes u_m can be obtained invoking with Δu_m, and the time-varying gain matrix $L(k)$ of the multiple harmonics disturbance observer can be solved.

3.3 Feasibility and stability analysis

Under the proposed MPC algorithm, the stability of the system (21) is given in the following.

Theorem 1: Considering the discrete-time system (21), the cost function is designed in (27) with constrains (28). The positive matrices V, Y, W and the predictive horizon n are chosen to calculate the optimal solution of the QP problem

$$
\min \frac{1}{2}\Delta U^T \Xi \Delta U + \Omega^T \Delta U \tag{32}
$$

s.t.

$$
E\Delta U \leq \Pi \tag{33}
$$

where ΔU, Ξ, Ω, E and Π are given in (31). Choosing the optimal cost function $\min J(k)$, then the nominal stable of the system (21) is guaranteed under the optimal solution.

Proof: For the QP problem (29) with constraints (30), let $\bar{p}^*$, Δu_m^* and γ^* be the optimal state, the optimal control input increment and the optimal relaxing factor, respectively. u_m^* is the optimal control input of u_m. Choosing

$$V^*(k) = \min J(k) \tag{34}$$

A sequence of the difference of the optimal control input is denoted as

$$\Delta\hat{u}_m^*(k) = [\Delta u_m^*(k|k), ..., \Delta u_m^*(k+n-1|k)]^T \tag{35}$$

which satisfies the constraints (28) and (30). The corresponding optimal sequence is denoted as

$$\hat{p}^*(k) = [\bar{p}^*(k+1|k), ..., \bar{p}^*(k+n|k)]^T \tag{36}$$

The optimal relaxing factor sequence is defined as follows:

$$\hat{\gamma}^*(k) = [\gamma^*(k+1|k), ..., \gamma^*(k+n|k)]^T \tag{37}$$

Consider the fact that the cost function $J(k)$ has been minimized by optimal input sequence, combined with (34), (35), (36) and (37), we have

$$V^*(k) = \min J(k) = \|\hat{p}^*(k)\|_{\bar{V}}^2 + \|\Delta\hat{u}_m^*(k)\|_{\bar{Y}}^2 + \|\hat{\gamma}^*(k)\|_{\bar{W}}^2 \tag{38}$$

According to equation (27), we have

$$\begin{aligned} J(k+1) = &\sum_{\vartheta=1}^{n} \|\bar{p}(k+\vartheta+1|k+1)\|_V^2 \\ &+ \sum_{\vartheta=0}^{n-1} \|\Delta u_m(k+\vartheta+1|k+1)\|_Y^2 \\ &+ \sum_{\vartheta=0}^{n-1} \|\gamma(k+\vartheta+1|k+1)\|_W^2 \end{aligned} \tag{39}$$

According to Ref. [17], if the predictive horizon n is selected sufficiently large, it has $\bar{p}(k+\vartheta+1|k+1) = \bar{p}^*(k+\vartheta+1|k)$, $\Delta u_m(k+\vartheta|k+1) = \Delta u_m^*(k+\vartheta|k)$ and $\gamma(k+\vartheta+1|k+1) = \gamma^*(k+\vartheta+1|k)$, $1 < \vartheta < n$. Then, it deduced that

$$\begin{aligned} J(k+1) = &\sum_{\vartheta=1}^{n} \|\bar{p}(k+\vartheta+1|k+1)\|_V^2 \\ &+ \sum_{\vartheta=0}^{n-1} \|\Delta u_m(k+\vartheta+1|k+1)\|_Y^2 \\ &+ \sum_{\vartheta=0}^{n-1} \|\gamma(k+\vartheta+1|k+1)\|_W^2 \\ = &\sum_{\vartheta=1}^{n} \|\bar{p}^*(k+\vartheta+1|k)\|_V^2 \\ &+ \sum_{\vartheta=0}^{n-1} \|\Delta u_m^*(k+\vartheta+1|k)\|_Y^2 \\ &+ \sum_{\vartheta=0}^{n-1} \|\gamma^*(k+\vartheta+1|k)\|_W^2 \end{aligned} \tag{40}$$

Further, it yields

$$
\begin{aligned}
J(k+1) = & \sum_{\vartheta=1}^{n} \|\bar{p}^*(k+\vartheta+1|k)\|_V^2 \\
& + \sum_{\vartheta=0}^{n-1} \|\Delta u_m^*(k+\vartheta+1|k)\|_Y^2 \\
& + \sum_{\vartheta=0}^{n-1} \|\gamma^*(k+\vartheta+1|k)\|_W^2 \\
= & \sum_{\vartheta=2}^{n} \|\bar{p}^*(k+\vartheta|k)\|_V^2 + \sum_{\vartheta=1}^{n-1} \|\Delta u_m^*(k+\vartheta|k)\|_Y^2 \\
& + \sum_{\vartheta=1}^{n-1} \|\gamma^*(k+\vartheta|k)\|_W^2 \\
= & \sum_{\vartheta=1}^{n} \|\bar{p}^*(k+\vartheta|k)\|_V^2 + \sum_{\vartheta=0}^{n-1} \|\Delta u_m^*(k+\vartheta|k)\|_Y^2 \\
& + \sum_{\vartheta=0}^{n-1} \|\gamma^*(k+\vartheta|k)\|_W^2 - \|\bar{p}^*(k+1|k)\|_V^2 \\
& - \|\Delta u_m^*(k|k)\|_Y^2 - \|\gamma^*(k|k)\|_W^2
\end{aligned} \tag{41}
$$

Combined with (38), it obtains

$$
\begin{aligned}
J(k+1) = & V^*(k) - \|\bar{p}^*(k+1|k)\|_V^2 \\
& - \|\Delta u_m^*(k|k)\|_Y^2 - \|\gamma^*(k|k)\|_W^2
\end{aligned} \tag{42}
$$

which means that $J(k+1) \leq V^*(k)$. Based on (38), it has $V^*(k+1) \leq J(k+1)$, then it yields

$$
V^*(k+1) \leq V^*(k) \tag{43}
$$

From (43), it illustrates that the Lyapunov function (34) is monotone decreasing, then the system (21) with MPC scheme is nominal stable. That means that the estimated errors of the disturbance observer is convergent, and the AMR (1) can track the UAV projection trajectory (2) with external disturbance. The proof is completed.

Remark 4 Combined with Theorem 1, after solving the QP problem (29), the control input schemes $u_m = u_m^*$ and the time-varying gain matrix $L(k)$ of the multiple harmonics disturbance observer are obtained. By combining $L(k)$ with equation (16), the disturbance estimated value can be calculated, hence the term u_d is obtained. Then, invoking with (1) and (12), the final control input $u = u_m + u_d$ for the AMR system can be obtained.

4 Experiment Results

In this section, the experimental results are presented, and the used experimental devices in experiment is produced by Quanser Corporation.

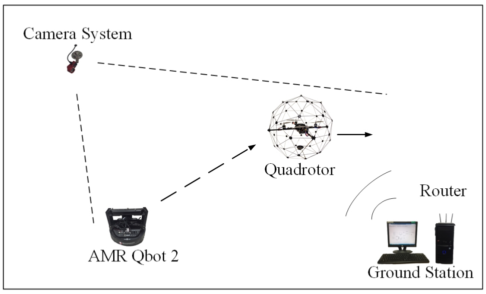

Fig. 4: The whole experimental environment

4.1 Parameters setup

The experimental platform in this paper consists of an AMR Qbot 2, an Optical-track camera system and a ground station with a router. The trajectory information of experimental devices is detected by the Optical-track camera system and interactively transferred to by the ground station with WLAN. The AMR device and experimental field are shown in Fig. 4. Restricted by the equipment, in this experiment, the AMR will track a virtual quadrotor UAV trajectory, and the used model of the quadrotor UAV is borrowed by Quanser Corporation.

Let the sample interval T as 0.02s, the initial position of the AMR are given that $x(0) = 0.4m, y(0) = 0.1m$. The projection initial position of the UAV are given that $x_r(0) = y_r(0) = 0m$, the desired linear velocity is $v_r(k) = 0.08m/s$, and the desired angular velocity $w_r(0) = 0.1rad/s$.

Combined with Theorem 1, to solve the parameters of the QP problem (29) with constraints (30), the weighting matrices are chosen as $V = 0.5 * I^{3\times3}, Y = 0.3 * I^{2\times2}$ and $W = 0.2 * I^{2\times2}$. The boundaries of the variables are chosen as $u_{m_{\min}} = [-0.1, -0.1]^T, u_{m_{\max}} = [0.1, 0.1]^T, \Delta u_{m_{\min}} = [-0.1, -0.1]^T$, $\Delta u_{m_{\max}} = [0.1, 0.1]^T$, $\bar{p}_{\min} = [0, -3, -3]^T$ and $\bar{p}_{\max} = [1, 3, 3]^T$. The boundaries of the relaxing factor coefficients are $c_{\min} = [-0.05, -0.05]^T$ and $c_{\max} = [0.05, 0.05]^T$. Besides, the parameters of the external disturbance are selected as follows:

$$
\begin{aligned}
Z_1 &= \begin{bmatrix} 0.9998 & -0.02 \\ 0.02 & 0.9998 \end{bmatrix}, Z_2 = \begin{bmatrix} 0.9992 & -0.04 \\ 0.04 & 0.9992 \end{bmatrix} \\
Z_3 &= \begin{bmatrix} 0.98 & -0.08 \\ 0.08 & 0.98 \end{bmatrix}, Z_4 = \begin{bmatrix} 0.92 & -0.12 \\ 0.12 & 0.92 \end{bmatrix} \\
Z_5 &= \begin{bmatrix} 0.88 & -0.16 \\ 0.16 & 0.88 \end{bmatrix}, Z_6 = \begin{bmatrix} 0.82 & -0.24 \\ 0.24 & 0.82 \end{bmatrix} \\
M_1 &= \begin{bmatrix} 0.2 & 0.2 \end{bmatrix}, M_2 = \begin{bmatrix} 0.8 & 0.8 \end{bmatrix} \\
M_3 &= \begin{bmatrix} 1 & 1 \end{bmatrix}, M_4 = \begin{bmatrix} 1.2 & 1.2 \end{bmatrix} \\
M_5 &= \begin{bmatrix} 1.6 & 0.6 \end{bmatrix}, M_6 = \begin{bmatrix} 0.4 & 0.4 \end{bmatrix}
\end{aligned}
$$

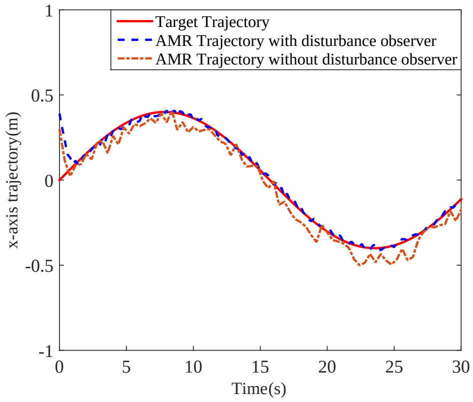

Fig. 5: x-axis tracking trajectory

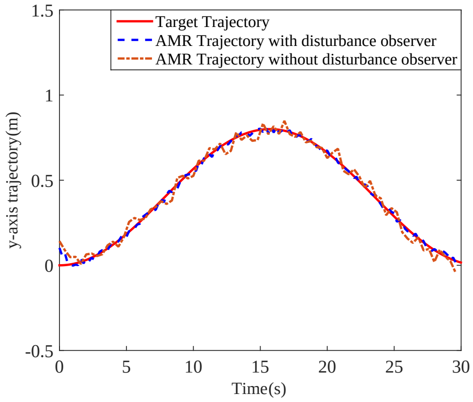

Fig. 6: y-axis tracking trajectory

4.2 Experimental results

In this part, let the virtual quadrotor as a tracked target, the experimental results are exhibited.

Figs. 5 and 6 show the AMR tracking trajectory at x-axis and y-axis. It can observe that without the disturbance observer, there are some deviations between the AMR trajectory and target trajectory, and the AMR can track the target trajectory effectively under the developed model predictive hybrid tracking control scheme based on the multiple harmonics disturbance observer. The tracking errors are shown in Fig. 7. It illustrates that the tracking errors are convergence. Fig. 8 presents the top view of the AMR trajectory with the tracked target trajectory. The target trajectory is a circle with 0.4m radius. Fig. 9 presents the actual space trajectory in the experimental field with the

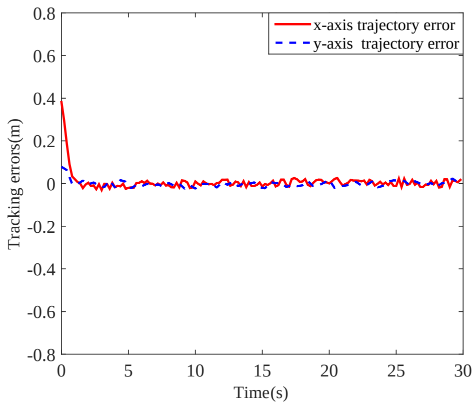

Fig. 7: The tracking errors of the AMR

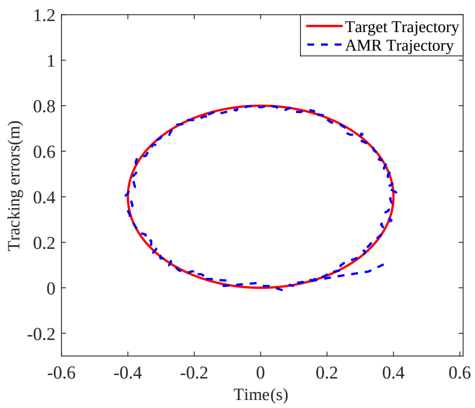

Fig. 8: Top view tracking trajectory of the AMR

virtual quadrotor. Fig. 8 and Fig. 9 validate that the AMR can effectively track the target trajectory.

From the experimental results, it obtains the proposed tracking control scheme under the proposed MPC method with the multiple harmonics time-varying disturbance observer is valid for the AMR.

5 Conclusion

In this paper, an air-ground hybrid tracking control scheme under the improved MPC method and multiple harmonics time-varying disturbance observer was proposed for the discrete-time nonholonomic AMR and UAV. By adopting the polar coordinate transformation method, a time-varying air-ground cooperative tracking control model had been presented. Considering the external

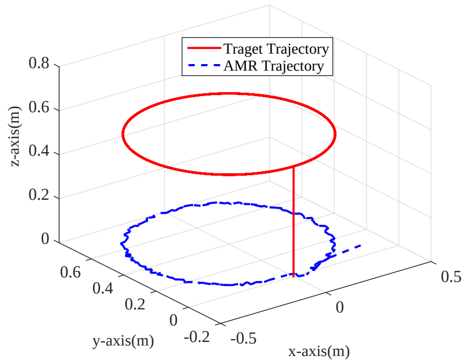

Fig. 9: Three dimension tracking trajectory

disturbance in tasks, a multiple harmonics time-varying disturbance observer had been designed for cooperative tracking. Then invoking with disturbance observer, the hybrid tracking control scheme had been solved by improved MPC method with relaxing factor. Finally, the experiments show the the effectiveness of the proposed tracking control scheme. The slipping, skidding, actuator fault and saturation in the AMR will be studied in the future.

6 Acknowledge

This work is supported in part by the National Nature Science Foundation of China under Grant 52105553, in part by Natural Science Research Start-up Foundation of Recruiting Talents of Nanjing University of Posts and Telecommunications under Grant No. NY221134.

7 Data availability

The datasets generated during and/or analyzed during the current study are available from the corresponding author on reasonable request.

8 Declarations

9 Conflict of interest

The authors declare that they have no known conflict of interest.

References

1. Wu, Y., Wang, Y., Fang, H.: Full-state constrained neural control and learning for the nonholonomic wheeled mobile robot with unknown dynamics. ISA Transactions. 12(2), 915–926(2021)
2. Wang, C., Ji, J., Miao, Z.: Synchronization control for networked mobile robot systems based on UdwadiaCKalaba approach. Nonlinear Dynamics. 105(1), 315–330(2021)
3. Yu, J., Liu, X., Gao, Y.: 3D channel tracking for UAV-Satellite communications in space-air-ground integrated networks. IEEE Journal on Selected Areas in Communications. 38(12), 2810–2823(2020)
4. Ding, R., Xu, Y., Gao, F.: Trajectory design and access control for air-ground coordinated communications system with multi-agent deep reinforcement learning. IEEE Internet of Things Journal. 46(7), 1005–1016(2021)
5. Radmanesh, M., Sharma, B., Kumar, M., PDE solution to UAV/UGV trajectory planning problem by spatio-temporal estimation during wildfires. Chinese Journal of Aeronautics. 34(5), 601–616(2021)
6. Qin, H., Meng, Z. Meng, W.: Autonomous exploration and mapping system using heterogeneous UAVs and UGVs in GPS-denied environments. IEEE Transactions on Vehicular Technology. 68(2), 1339–1350(2019)
7. Xue, Z., Wang, J., Ding, G.: Cooperative data dissemination in air-ground integrated networks. IEEE Wireless Communications Letters. 8(1), 209–212(2019)
8. Wang, Z. McDonald, S.: Convex relaxation for optimal rendezvous of unmanned aerial and ground vehicles. Aerospace Science and Technology. 27(5), 1018–1027(2020)
9. Cheng, W., Jiang, B., Zhang, K.: Robust finite-time cooperative formation control of UGV-UAV with model uncertainties and actuator faults. Journal of the Franklin Institute. 358(17), 8811–8837(2021)
10. Cajo, R., Thi, T., Plaza, D.: A survey on fractional order control techniques for unmanned aerial and ground vehicles. IEEE Access. 60(7), 988–1000(2019)
11. Chen, M. Disturbance attenuation tracking control for wheeled mobile robots with skidding and slipping. IEEE Transactions on Industrial Electronics. 64(4), 3359–3368(2017)
12. Zhang, B., Song, Y.: Efficient model predictive control for Markovian jump systems with Lur'e nonlinear term: A dual-mode control scheme. International Journal of Robust and Nonlinear Control. 32(5), 2603–2623(2022)
13. Britzelmeier, A., Gerdts, M.: A nonsmooth Newton method for linear model predictive control in tracking tasks for a mobile robot with obstacle avoidance. IEEE Control Systems Letters. 20(1), 257–265(2020)
14. Hou, R., Cui, L., Bu, X.: Distributed formation control for multiple nonholonomic wheeled mobile robots with velocity constraint by using improved data-driven iterative learning. Applied Mathematics and Computation. 395(1), 495–503(2021)

15. Wang, D., Wei, W., Yao, Y.: A robust model predictive control strategy for trajectory tracking of Omni-directional mobile robots. Journal of Intelligent and Robotic Systems. 98(2), 439–453(2020)
16. Lafmejani, A., Berman, S.: Nonlinear MPC for collision-free and deadlock-free navigation of multiple nonholonomic mobile robots. Robotics and Autonomous Systems. 61(12), 1502–1515(2021)
17. Li, J., Yang, C., Su, C.: Vision-Based model predictive control for steering of a nonholonomic mobile robot. IEEE Transactions on Control Systems Technology. 24(2), 553–564(2016)
18. Dai, L. Lu, Y., Xie, H.: Robust tracking model predictive control with quadratic robustness constraint for mobile robots with incremental input constraints. IEEE Transactions on Industrial Electronics. 68(10), 9789–9799(2021)
19. Ding, S., Chen, W. Mei, K.: Disturbance observer design for nonlinear systems represented by input-output models. IEEE Transactions on Industrial Electronics. 67(2), 1222–1232(2020)
20. Chen, M., Ren, Y., Liu, J.: Antidisturbance control for a suspension cable system of helicopter subject to input nonlinearities. IEEE Transactions on Systems, Man, and Cybernetics: Systems. 48(12), 2292–2304(2018)
21. Zhang, Q., Dong, J.: Disturbance-observer-based adaptive fuzzy control for nonlinear state constrained systems with input saturation and input delay. Fuzzy Sets and Systems. 392(1), 77–92(2020)
22. Yan, Y., Yang, J., Sun, Z.: Non-linear-disturbance-observer-enhanced M-PC for motion control systems with multiple disturbances. IET Control Theory and Applications. 14(1), 63–72(2020)
23. Liu, C., Chen, W., Andrews, J.: Tracking control of small-scale helicopters using explicit nonlinear MPC augmented with disturbance observers. Control Engineering Practice. 20(3), 258–268(2012)
24. Sun, Z., Xia, Y., Dai, L.: Disturbance rejection MPC for tracking of wheeled mobile robot. IEEE/ASME Transactions on Mechatronics. 22(6) 2576–2587(2017)
25. Chen, M., Xiong, S., Wu, Q.: Tracking flight control of quadrotor based on disturbance observer. IEEE Transactions on Systems, Man, and Cybernetics: Systems. 354(10), 1–10(2019)
26. Bhatia, A., Jiang, J., Zhen, Z.: Projection modification based robust adaptive backstepping control for multipurpose quadcopter UAV. IEEE Access. 7(1), 154121–154130(2019)
27. Li, W., Ding, L., Liu, Z.: Kinematic bilateral teledriving of wheeled mobile robots coupled with slippage. IEEE Transactions on Industrial Electronics. 64(3), 2147–2157(2017)
28. Nie, J., Wang, Y., Miao, Z.: Adaptive fuzzy control of mobile robots with full-state constraints and unknown longitudinal slipping. Nonlinear Dynamics. 106(4), 3315–3330(2021)
29. Yang, H., Guo, M., Xia, Y.: Trajectory tracking for wheeled mobile robots via model predictive control with softening constraints. IET Control Theory and Applications. 12(2), 206–214(2018)

30. Begnini, M., Bertol, D., Martins, N.: A robust adaptive fuzzy variable structure tracking control for the wheeled mobile robot: Simulation and experimental results. Control Engineering Practice. 64(2), 27–43(2017)
31. Kong, L., Yuan, J.: Generalized discrete-time nonlinear disturbance observer based fuzzy model predictive control for boiler - turbine systems. ISA transactions. 90(12), 89–106(2019)